PHASE GRATINGS AS LO-DISTRIBUTORS IN SUBMM HETERODYNE ARRAYS

T.KLEIN, G.A.EDISS, R.GÜSTEN, C.KASEMANN
MPIfR-Bonn, Auf dem Hügel 69, 53121 Bonn, Germany
email: tklein@mpifr-bonn.mpg.de

ABSTRACT

Phase gratings have found an important application in the submm wavelength range with the development of heterodyne arrays in the past few years. These devices can be used as efficient beam splitters to match the signal beam of a single local oscillator source to an array of detector devices such as SIS-mixers or HEBs. Here we report on a phase grating developed for CHAMP - the **C**arbon-**H**eterodyne-**A**rray of **MP**IfR - which is currently operating at the Caltech Submillimeter Telescope on Mauna Kea [1]. For further applications, such as heterodyne arrays for higher frequencies, we continued our work on designing phase gratings to enhance their efficiencies and to provide solutions for future array projects. Here we report on an algorithm we have developed as a design tool for phase gratings providing solutions for any desired array, nearly independent on the desired beam configuration.

Introduction

The periodic modulation of the amplitude and (or) the phase of an electromagnetic wave generates a set of waves, called diffraction orders, propagating in discrete directions. Devices stimulating these effects are well known as diffraction gratings for the visible region of the electromagnetic spectrum. A scalar formulation of diffraction at a periodic structure modulating an incident wave can be expressed in Fourier optics [2] by the complex Fourier transform

$$A(x,y) = \int_{-\infty}^{\infty}\int_{-\infty}^{\infty} b(x',y') \cdot t(x',y') \cdot e^{\frac{-2\pi i(xx'+yy')}{\lambda f}}\, dx'\, dy' \qquad (1)$$

in which the complex field b(x',y') of the incident wave is modulated by the periodic structure as expressed by the transmission function t(x',y'). The distribution of the diffracted field $A(x,y)$ appears in the focal plane of the transforming lens with focal length f. The wavelength λ and f, which is the distance between the structure and the lens appear as scaling factors in the equation. (x,y) and (x',y') are the coordinates in the object and frequency domain related by the transform.
With this equation the determination of the grating structure is reduced to the calculation of $t(x',y')$, which is the result of the inverse Fourier transform. In case

of

$$|t(x', y')|^2 = \frac{|a(x', y')|}{|b(x', y')|} = 1 \tag{2}$$

a phase only modulation is achieved. If the complex field of the incident wave and the desired intensity distribution in the far field is determined by the specific application, the transmission function has to be found which fulfills the condition (2). The result of this consideration is that in case of a phase only modulation there is no direct analytic solution of the problem but an iterative way of calculating equation (1) can be found.

In the following two methods are considered leading to a solution of the problem. Both are based on the equations mentioned above. The method considered first was given by *Dammann and Klotz* [4]. Here the set of possible transmission functions is reduced by a quantisation of the phase levels and a limitation in the number of transition points where the function changes from one phase level to another. An additional reduction can be achieved by taking into account given symmetries of the specific application. How this method can be realised numerically is reported in several publications [4] [5] [6] [7]. Here we focus on a solution of such a grating implemented in the CHAMP LO-optics.

A second method is based on a so called *Phase-Retrieval Algorithm*, which uses the known functions in eq.(1), $\|A(x, y)\|$ and $b(x', y')$, as well as an initial estimate for the far field distribution of the phase of $A(x, y)$, to calculate the inverse FFT to obtain $t(x', y')$, belonging to $b(x', y')$. This Fourier pair then leads, after the calculation of the FFT, to a new and better estimate for the far field phase of $A(x, y)$, giving the initial function for the next iteration.

The idea of this algorithm was given by *Gerchberg and Saxton* [8] and has been applied in areas where phase information has to be found out of single intensity measurements. The method has been adapted to find the transmission function for a given grating problem.

THE DAMMANN METHOD

The main simplification in Dammann's method is the separation of the two-dimensional transmission function into a set of two one-dimensional functions. The combination of such one-dimensional solutions can only lead to a regular grid array of $K \times N$ beams. Table I lists the obtained efficiencies for chosen values K and N, which are binary or with 4 allowed phase levels Φ between the transition points. With the higher level gratings the efficiency can be increased significantly as shown in the table. Although with the chosen even symmetry for the grating period it is impossible to generate the array configuration of a CHAMP-subarray, we used the found solutions for K=3 and K=4 with four phase levels to couple 8 of the 12 generated beams to the subarray. The FFT according to eq. (1) is shown in fig.I for the given problem. The grating structure (blue curve) is illuminated by a gaussian beam (left figure). For simplicity, the grating should be positioned at the waist of the illuminating beam so that the phase of the incident wave can be assumed to be flat. The beamwaist, ω_0, should have the same size as the period of the grating as mentioned in [3]. However changing the size of the beamwaist within $\omega_0 \geq d/2$ does

TABLE I Efficiencies of two-dimensional gratings, binary and four-level type in comparison

	2×2	3×3	4×4	5×5	3×4	3×5	4×5
binary	65.8%	44.1%	50.0%	59.4%	46.9%	51.2%	54.5%
4-level		80.3%	68.9%	74.0%	74.4%	77.1%	71.4%

not affect the results significantly because the information remains in the real and imaginary parts (fig.I). If the beamwaist becomes smaller than d/2 more and more information gets lost. In the worst case the complete wave is delayed by the same value which couples the energy only into the zero diffraction order.
The result of the transformation is shown in the real and imaginary part in fig.I, as well as the calculated amplitude and phase of the diffracted field. As the transmission function and the illuminating beam are of even symmetry, amplitude and phase of the image are also even functions. However it is also possible to generate even symmetric images with an odd symmetric transmission function (translation symmetry). In this case the zero diffraction order is rejected because the symmetry implies a transition point at the center of the period [9].

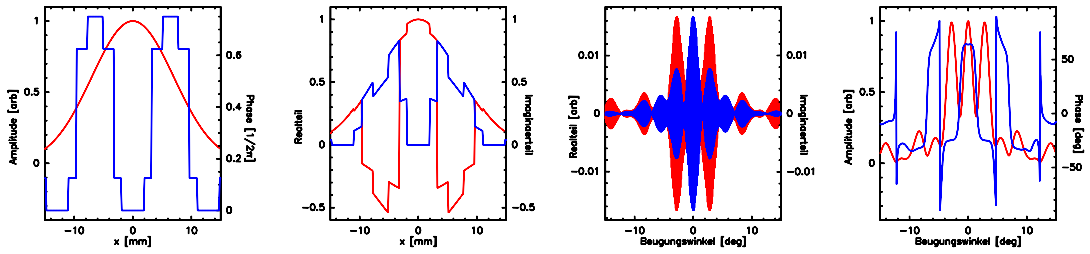

FIGURE I A gaussian beam illuminating a grating surface (4-level type) is shown in the left picture. The next graph shows the modulated amplitude (real and imaginary part) as it is transformed. The resulting real and imaginary part of the diffracted field is shown in the following graph. Finally the intensity and phase of the generated image shows an array of 3 beams.

Realisation

The fabrication of the surface structure on the material PTFE has been made with a nc-machine in the workshop of our institute. PTFE has been chosen because its refraction index at submm wavelengths minimizes the reflections at the surfaces. The machining of this material however is difficult due of the smoothness of this material. Instead of combining the one-dimensional solutions by adding the phase structures and realizing the complicated structure on the PTFE surface we fabricated a grating layer of each one-dimensional solution and combined the physical

layers to a two-dimensional device. This method has the advantage that only grooves have to be machined on the material. In addition each layer can be characterized in the experiments and can be combined with various other layers.
Fig.II shows photographs of the two types of fabricated layers, each of them as a one-dimensional grating. For an accurate combination of the layers there is a reference edge on each layer to achieve the desired two-dimensional phase delay. Fig.III

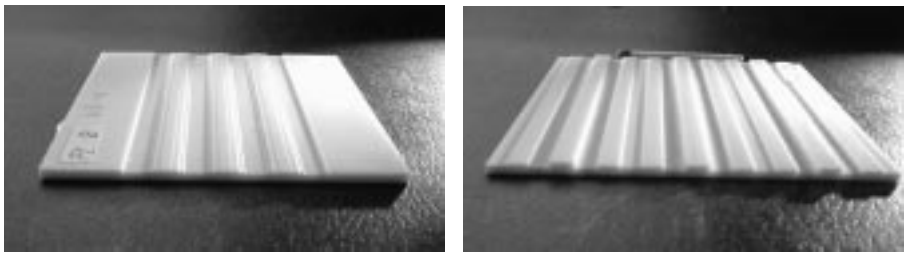

FIGURE II Photographs of both PTFE-layers fabricated on a nc-machine. The left photo shows the grating generating a linear 3-beam array, the photo on the right shows the equivalent grating for a 4-beam array. The square PTFE-plates have a length of 80mm. Each of them carries 3 periods of the specific structure.

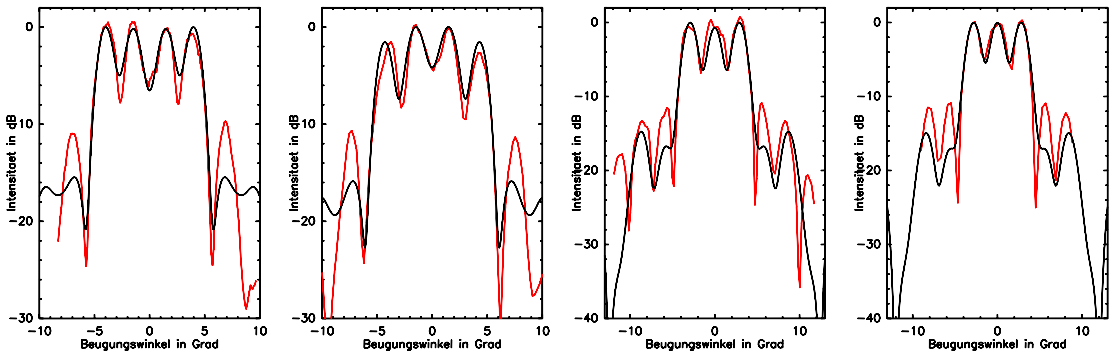

FIGURE III Results of the antenna measurements (red) in comparison with the theoretical expected intensity distributions. (black) at 460.2GHz (left) and 492GHz (right) for each of the grating layers. The results are in good agreement with the theory. Only for the higher orders differences of about 10% occur.

shows the experimental results compared to what is expected from theory. The generated linear arrays with 3 and 4 beams completely agree with the theory in order of the accuracy of measurement. Only differences are that the higher orders are seen at the 10% level. This shows that any effects to the assumption of a real gaussian illumination without any variation in phase of the incident beam are negligable in case of the potter horn antenna used in the experiment.
With measurements at various frequencies, 460.2GHz ($\triangle\nu_{center} = 15GHz$) and

492GHz ($\triangle\nu_{center} = 17GHz$) the frequency dependence of the gratings could be verified. The expected change of the diffraction angles, as well as of the relative intensities are shown by the experiment. Fig.IV shows the intensity measurements for several combinations of the two solutions, 3×3, 4×4 and 3×4 arrays. Because the experiments are based on the heterodyne detection of the signals, an accurate experimental value for the achieved efficiency cannot be given here, as the measurement of the detected power with and without the devices is required which implies different beam coupling between the signal source and heterodyne receiver. However the accurate scaling of the parameters for the phase delay is indicated by the rejection of the zero order by more than 20dB in case of the 4×4 array. After the

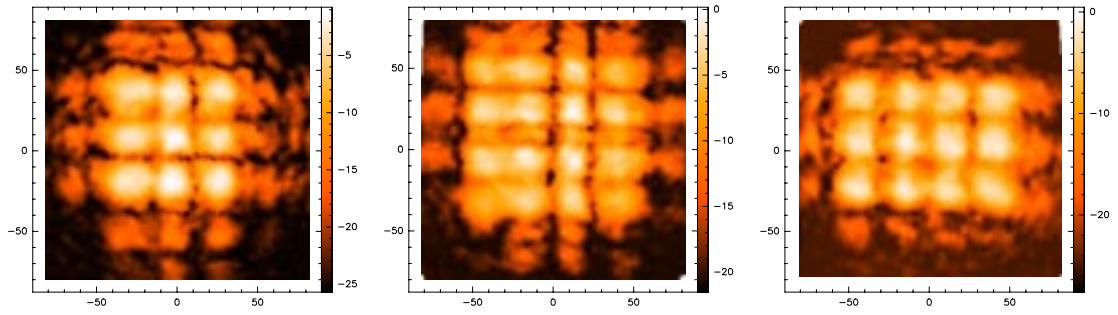

FIGURE IV Two-dimensional diffraction spectra for combined grating layers for K=3 and K=4. Coordinates are given in mm. The measured intensities are shown in a dB scale.

measurements of the generated intensity distributions it also has to be verified that the device is able to couple a suitable amount of power to an array of SIS-mixers. For this test the components of the CHAMP L.O. system have been set up on an optical frame as shown in fig. VI.
The output power of the frequency stabilized gunn oscillator is adjustable by a mechanical attenuator to vary the power injected into the mixer. A potter horn antenna couples the rf-output of the multipliers to free space generating a beamwaist of 1.1mm. A HDPE lens transforms this waist (7mm) to one at the input of the gaussian telescope lens pair. The intermediate waist (16mm) of the gaussian telescope, $2f$=900mm, illuminates the phase grating mounted at the waist position. The generated signal array was then coupled into a SIS mixer device via a Martin-Puplett-Interferometer which could be moved together with the mixer to each array matrix position. The IV-curves then monitored the detected L.O. signal. Starting with one position the L.O. signal power was adjusted to obtain a minimum noise temperature for the mixer. It was seen that the injected L.O. power gave a huge margin because the mixer showed a typical normal resistance feature indicating a sufficient coupling efficiency. After attenuating the power for maximum mixer performance on one position, the noise temperatures for each array position was measured and compared.
The measured iv-curves as well as the total power responses for the noise measurements at a frequency of 492GHz are shown in fig. V, according to the position in

the subarray. The differences in injected L.O. power was indicated by the noise performance variation to be less than 10%.
The described technique of testing the device operating as a L.O. injection system has the advantage of being independent of the mixer's characteristics by using the same mixer for all measurements. Otherwise the results would include the individual behaviour of each mixer, such as its sensitivity to the L.O. signal caused by the individual backshort adjustment or like the individual noise performance itself. Therefore the measured noise temperature variation here characterizes only the functionality of L.O. injection.

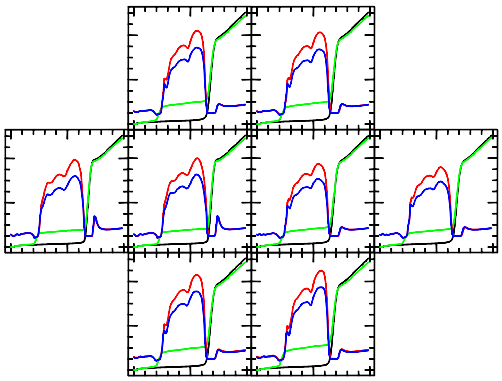

FIGURE V Current/voltage and power/voltage curves of the mixer at various subarray positions. To be independent of the variable characteristics of several mixers the curves are obtained by a single mixer moved to the various positions of the subarray detectors.

FIGURE VI CHAMP L.O. optics. With folding both optical paths the system could be integrated on a mounting plate of 1m in diameter. In the foreground one of the two L.O. sources is visible. The grating is mounted under the gold plated flat mirror injecting the signals into the cold optics of CHAMP.

THE PHASE-RETRIEVAL ALGORITHM

As mentioned in the previous section the Dammann method can only provide solutions for regular matrix arrays because of the required separableness of the transmission function. In case of non regular arrays a full two-dimensional consideration of eq. 1 is necessary. Hence we apply a phase retrieval algorithm, recovering the phase of an object out of the information given by the intensity distributions of the desired image and the illuminating beam. This method is based on the idea of *Gerchberg and Saxton* [8] and therefore often called *Gerchberg-Saxton-Algorithm*. The principle of the algorithm is to Fourier transform between the two domains back and forth changing the functions in a way that they fulfill the constraints given by the required beams. The adaptation of this principle to the foregoing grating problem is formulated in fig.VII. The algorithm is starting with the desired intensity distribution and a first guess for the phase distribution Φ_0 of the complex field. Transforming

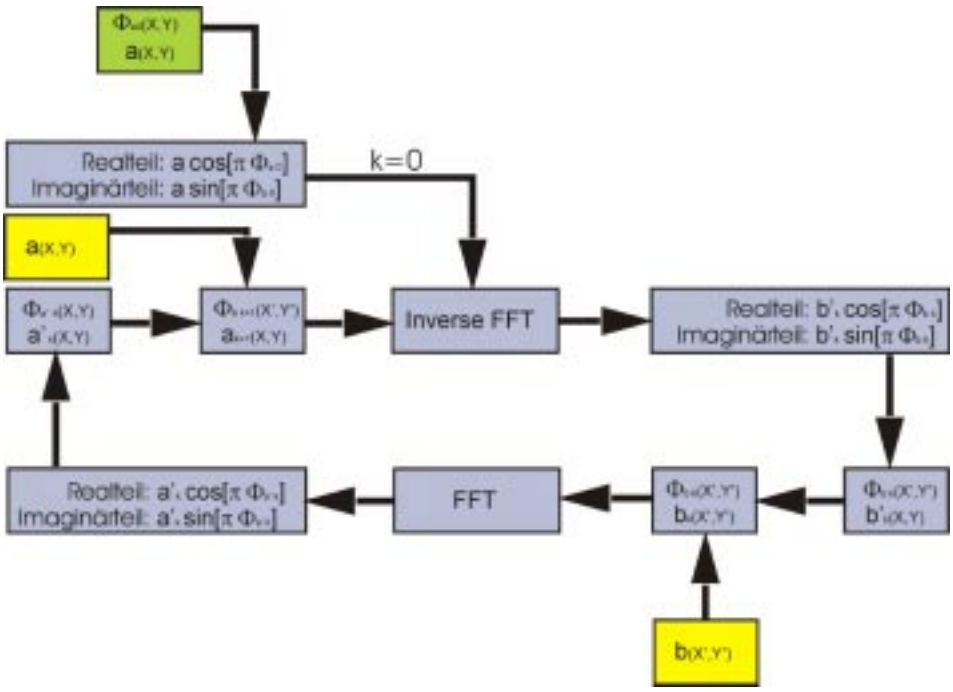

FIGURE VII Flow chart of the algorithm for the grating problem. After initialization of the image with $a(x, y)$ and $\Phi_{a0}(x, y)$ (green) the algorithm starts with an inverse FFT. In the object domain $b_k(x', y')$ is replaced by the illumination function $b(x', y')$ (yellow), after the FFT $a'_k(x, y)$ is replaced by the desired image $a(x, y)$ (yellow). With a monotone decrease of the error function $a'_k(x, y)$ approximates a solution.

this function via an inverse complex two-dimensional FFT yields phase and amplitude distributions in the object domain where the grating is located. The amplitude however does not fulfill the requirement for a gaussian illumination due to the fact that the phase only modulation is a special case of solution. Therefore the amplitude $b'_k(x', y')$ has to be replaced by the the desired illumination of gaussian shape $b(x', y')$ before transforming back. After the FFT a result for the diffraction image is obtained. The efficiency and the differences are calculated to monitor the current status of the results. Before starting the next iteration the amplitude of the diffraction image is replaced by the desired intensity distribution. The phase remains as a new estimate for the next iteration.
The FFT treats the functions in discrete form as

$$A(x, y), B(x', y') \rightarrow A(m, n), B(p, q)\,, \text{described by} \tag{3}$$

$$A_{mn} = \frac{1}{MN} \sum_{p=0}^{M-1} \sum_{q=0}^{N-1} B_{pq} e^{-2\pi i \frac{qm}{M}} e^{-2\pi i \frac{pn}{N}} \tag{4}$$

is the discrete formulation of eq. (1) as considered in [10].
To characterize the transmission function, merit functions are calculated by

$$\eta_k = \frac{\sum\limits_p \sum\limits_q a'_{pq}}{\sum\limits_m \sum\limits_n a_{mn}}\,, \tag{5}$$

giving the efficiency achieved at the kth iteration the grating efficiency, and an error function ϵ_k

$$\epsilon_k = \frac{1}{M \cdot N} \frac{\sum\limits_{m=0}^{M} \sum\limits_{n=0}^{N} [a'_{mnk} - a_{mn}]}{\sum\limits_{m=0}^{M} \sum\limits_{n=0}^{N} a_{mn}^2}\,, \tag{6}$$

indicating how the intensity in the desired orders is equalized.

Realization

The algorithm has been realized on a HP-UNIX workstation which operates two fast processors and provides sufficient memory for the huge amount of data. The main part of the program is a routine for the two-dimensional FFT which has been derived from *Numerical Recipes in C* [10]. However the routine was slightly modified to a higher accuracy because rounding errors with the original routine led to significant effects during many iterations.
The data, two-dimensional arrays, have sizes $2^N \times 2^M$. The FFT itself has then to treat 2^{N+M+1} array values. The time the computer needs for a single iteration is minimized by careful choice of values for N and M which includes a consideration of a useful sampling of data [11] to avoid aliasing. The results presented in the following were calculated with M, N=9 which was related to a computing time of 10 seconds per iteration and a memory allocation of 31MB. The program follows in principle the steps of the flow chart given in fig. VII. In addition the values for the efficiency and error are calculated. An integrated module gives the option to determine an order of quantisation of the transmission function and to change this order during the algorithm iterations to implement practical constraints given by the mechanical fabrication procedures.

Results

The first problem solved by the algorithm is the 2-4-2 configuration of a CHAMP subarray. As mentioned the data arrays were dimensioned as 512×512 pixel arrays. The offsets for the desired diffraction orders a_{mn} are ±16 and ±48 pixel in the main axis and ±32 pixel in the second axis of the array. The widths of the gaussians are 12 pixels. Fig.VIII shows the results for several phases during iteration. The left column lists the grating structures Φ_{bpq}, the column in the middle lists the generated intensity distribution a'_{mn} and the far field phase is listed in the right column of the figure. The top row shows the result after the 1st, the 5th and the 30th iteration. As indicated by this sequence the intensities in the undesired higher orders are more and more reduced by further iterations. The monotone decrease of

the error becomes visible considering the intensity distributions of fig.VIII, after 30 iterations the intensity is distributed equally over the desired orders of the array. Up to 5 iterations, there are diffraction orders visible between the desired orders indicating that all even orders are rejected as stimulated by the even symmetry of the transmission function. Indeed the initial estimate for the phase distribution in the far field has been chosen to be even which makes the complex initial function for the first FFT symmetric. This has been done to force the algorithm to find a solution on a short time scale. Using another estimate, such as a random distribution for the initial phase, yields similar results but increases the number of iterations needed by a factor of 10. It is obvious that the values for the error function have a strong dependence on the chosen initial phase distribution.

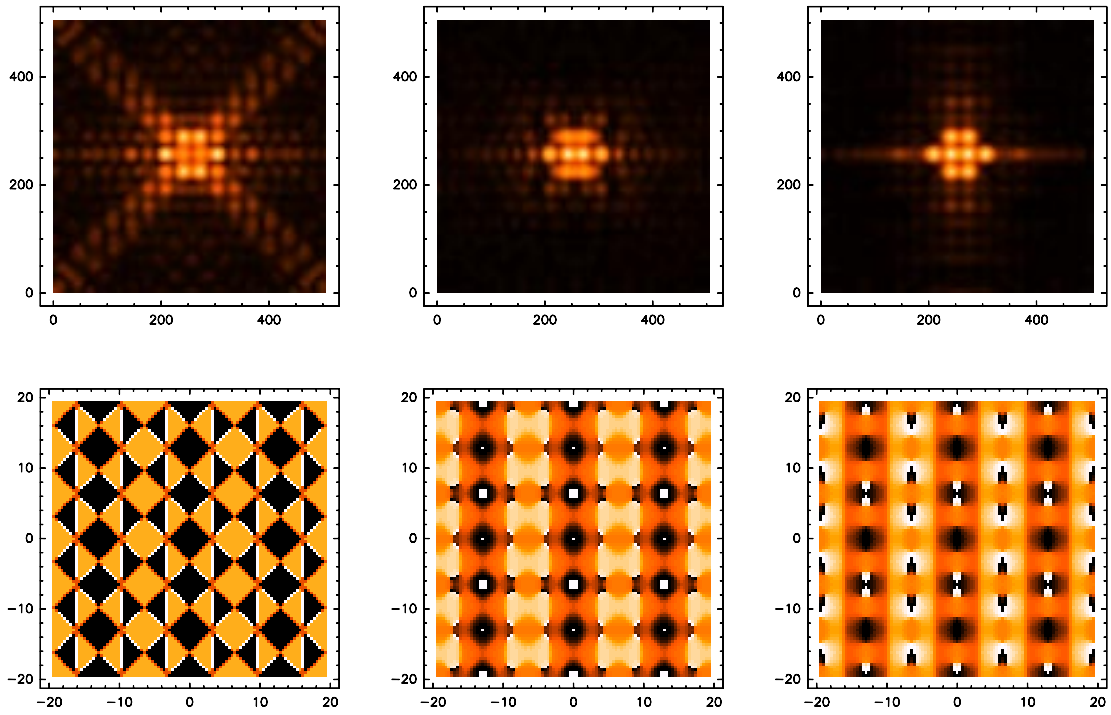

FIGURE VIII Intensity (top) and phase modulation (bottom) after 1,5 and 30 iterations (left to right) of the algorithm. Colours are scaled from zero (black) to 2π (white) and zero to unit for intensity.

Quantisation of phase levels

Simplifying the phase structure can be advantageous for a physical realization of the application of such solutions. Therefore the program is able to implement an order of quantisation of the phase levels (l=2,4,8,16,...). After each iteration the resulting phase distribution is digitized as:

$$\Phi_{kmn} \rightarrow \frac{2\pi}{l} \cdot s\,, \tag{7}$$

with s as an integer in the range 0 to l chosen that

$$\Phi_{kmn} - \frac{2\pi}{l} \cdot s = min\,. \tag{8}$$

Fig. IX shows the results obtained for several quantisation levels. Although the algorithm is limited by the strong quantisation, reasonable results can be obtained. As expected, the more the phase structure is simplified by the chosen order of quantisation the less the efficiency and the higher the value of the error function (see fig. X) is obtained. A digitization to 8 phase levels seems to be possible without significant changes in the devices performance. Going to 4 allowed phase levels there is a significant increase on the error function and the efficiency is limited to 68%. Better results were obtained when the digitization started later after 15 iterations as it is indicated by the dashed lines in fig. X. With this method the results for a four level structure is similar to a 32 level type. In conclusion it is shown that it is possible to simplify the phase structure without significantly changing the performance. This makes the described method interesting for application in practice. Other array

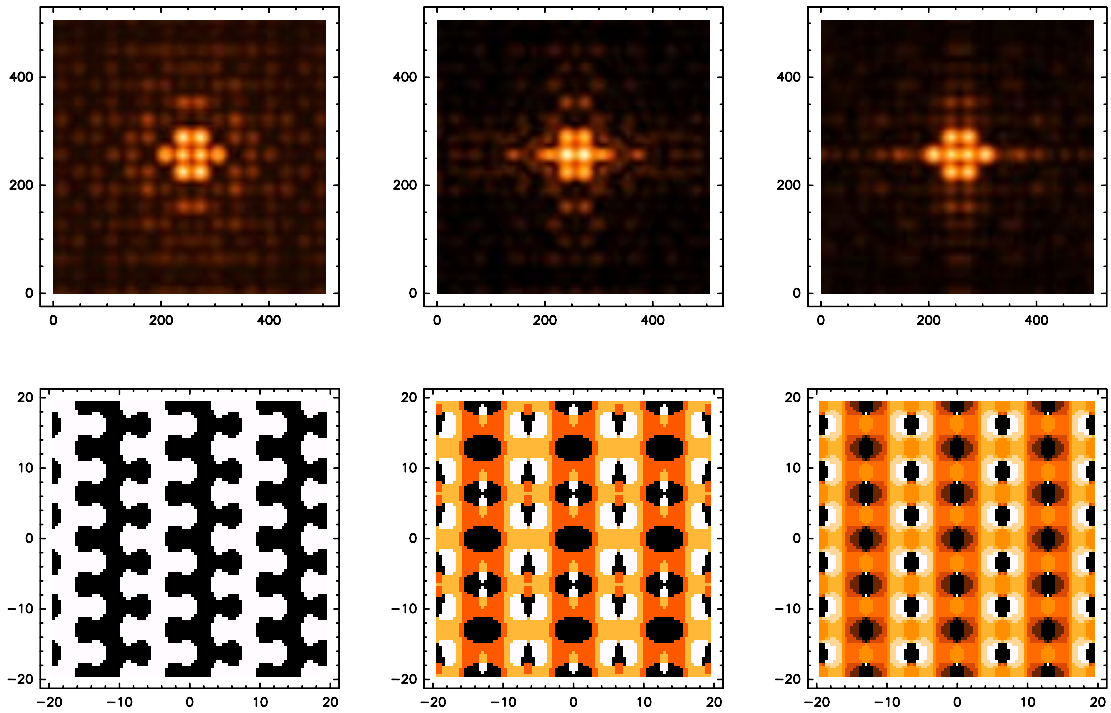

FIGURE IX Generated intensity distributions for 2,4 and 8 discrete phase levels and the resulting grating surfaces (below) are shown. For the binary case the algorithm leads to a translation symmetric transmission function which achieves a significantly better result than for the 4-level type. The 8-level type has nearly the same performance as a non digitized solution (less than 10% decrease of efficiency).

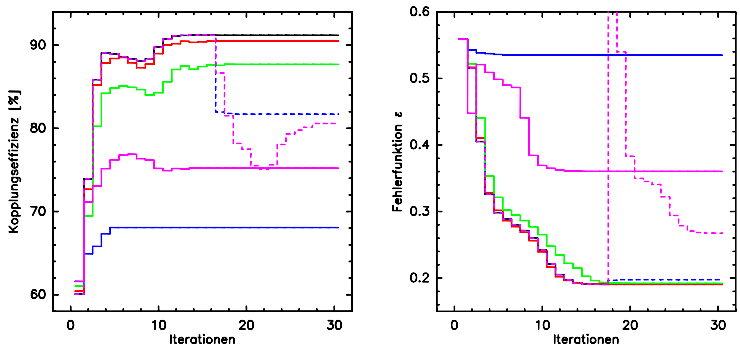

FIGURE X Convergence of the algorithm for 2 (pink), 4 (blue), 8 (green), 16 (black) and 32 (red) allowed phase levels. The left graph shows the grating efficiency, the right graph shows the error function. Digitization was performed at the start of the algorithm except for the dashed lines digitization started after 15 iterations yielding better results.

configurations can be easily calculated because the algorithm only requires for the initial function given by the desired array. Some examples are shown in fig.XI. During testing the algorithm a variety of configurations have been calculated without discovering any limits of this method.

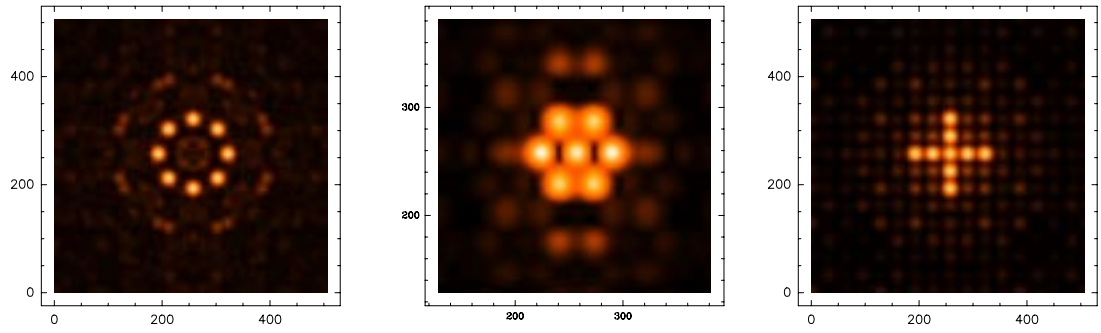

FIGURE XI Some examples of grating solutions for array generation. Between the more exotic configurations, as a circle or a cross, the hexagonal configuration of beams is often used for array receivers. The extension for more beams is possible. In case of the circle the O^{th} diffraction order has been very well rejected.

Distributions without symmetries

In the following we consider an intensity distribution which has no kind of symmetry. The interesting difference here to the previous calculations is that a desired intensity which can be considered as a frequency in the image domain according to its offset does not have an identical intensity at the same negative frequency.

A photograph [1], has been digitized as the desired image to be generated by an illuminated phase grating. Fig.XII shows the result for the generated image after 1500 iterations on the left which can be compared to the original image on the right side of the figure. The result is a surprisingly accurate reproduction of the desired image. Only 2% of the intensity is coupled to the outer region not belonging to the image. The size of the original 164×180 pixels is according to 29520 diffraction orders in the image domain. The data field for the calculations had a size of 1024×1024 (allocating 123MB of workspace) to avoid aliasing. This huge number of diffraction orders is mirrored in the phase structure of the grating shown in the center of fig.XII as a fine structured distribution. The variation of the phase seems not to have any order of direction as it is to be expected from the original image. But it becomes visible in the graph that there are two structures overlaid, a fast changing structure (dark blue and white) and a second with a smooth variation in phase.

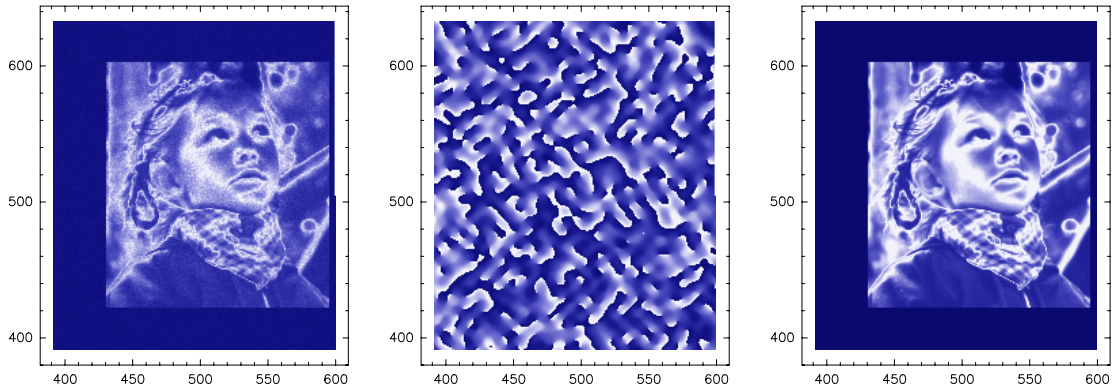

FIGURE XII The picture on the right shows the original picture a photo with a resolution of 164×180 pixels to be generated by a holographic phase structure. This structure is shown at the center of the figure as a result after 1500 iterations of the algorithm. On the left the generated image is presented, a surprisingly accurate reproduction of the original.

Outlook

We reported on the successful application of phase gratings as quasi-optical local oscillator beam splitter as used for our heterodyne array receiver CHAMP. The transmission gratings fabricated of PTFE were calculated by use of the Dammann Method. The experiments and, finally, their implementation in a working system, demonstrate that this type of device provides solutions for a variety of array receiver systems in the submm- and terahertz region for the future. With the phase

[1]The photo shows the author's three year old daughter

algorithm, as reported here, gratings can be calculated for every type of beam configuration, especially for non regular arrays. A first prototype for this kind of grating is planned for the near future as it is foreseen for the CHAMP-D project [12], a copy of the existing system covering the 450μm window of the atmosphere.

REFERENCES

[1] R.Güsten, G.A.Ediss, F.Gueth, K.H.Gundlach, H.Hauschildt, C.Kasemann, T.Klein, J.W.Kooi, A.Korn, I. Krämer, H.G.LeDuc, H.Mattes, K.Meyer, E.Perchtold, M.Pilz: "CHAMP: the Carbon Heterodyne Array of the MPIfR", Proc. SPIE Vol.3357, pp.167-177, Advanced MMW, Radio, and Terahertz Telescopes, 1998

[2] J.W. Goodman: "Introduction to Fourier Optics", McGraw-Hill, New York,1968

[3] J.A. Murphy, S.Withington, M. Heanue: "Local Oscillator Splitting Using Dammann Phase Gratings" Proceedings of the 3rd Interational Workshop on Terahertz Electronics, Zermatt, 1995

[4] H.Dammann, E.Klotz: "Coherent optical generation and inspection of two dimensional periodic structures", Optical Acta, Vol 24, No.4, pp.505-515, 1977

[5] S.J. Walker, J. Jahns: "Array generation with multilevel phase gratings", J. Opt. Soc. Am., Vol 7, No.8,1990

[6] T. Klein, G.A. Ediss, R. Güsten, H. Hauschildt, C. Kasemann: "Local Oszillator Beam Array Generation at 480GHz by Use of Phase Gratings", 8th International Symposium on Space Terahertz Technology, Harvard-Smithsonian Center for Astrophysics, Cambridge MA,1997

[7] T. Klein: "Entwicklung diffraktiver Beamsplitter und Integration der Systemoptik fuer ein Submillimeter Heterodyn Array", PhD thesis, MPIfR Bonn, 1999

[8] R.W. Gerchberg and W.O. Saxton, Optik 35, 237, 1972

[9] R.L. Morrison: "Symmetries that simplify the design of spot array phase gratings", J. Opt. Soc. Am. A, Vol. 9, No. 3, 1992

[10] W.H. Press, S.A. Teukolsky, W.H. Vetterling, B.P. Flannery: "Numerical Recipes in C", chapter 12, pp.521-525, Cambridge University Press, 1992

[11] W.H. Press, S.A. Teukolsky, W.H. Vetterling, B.P. Flannery: "Numerical Recipes in C", chapter 12.1, pp.500-502, Cambridge University Press, 1992

[12] Space Research Organisation Netherlands: "A SRON-MPIfR 16-element Heterodyne array receiver for the 625-720 GHz (D-band) atmospheric window", http://www.strw.leidenuniv.nl/jcmt/champ.html